Drop Size Distribution in Agitated Liquid-Liquid Systems

HSIAO TSUNG CHEN and STANLEY MIDDLEMAN

University of Rochester, Rochester, New York

The drop size distributions resulting from the agitation of immiscible liquids were measured over a wide range of parameters. The average drop size is correlated by $\overline{D}_{32}/L = 0.053\ N_{We}^{-0.60}$. The distribution function for volume fraction is normal and depends only upon $\overline{D}_{32}$. The results are valid for very dilute solutions wherein coalescence of droplets plays no role in the dispersion mechanism.

The prediction of interfacial area in agitated dispersions is of considerable importance in heat and mass transfer operations and in certain heterogeneous reactions. Rietema (*11*) discusses control of reaction rate in a stirred-tank reactor through control of drop size and interfacial area. Interfacial area control also plays an important role in liquid-liquid extraction (*15*), dispersion polymerization (*7, 8*), and direct-contact heat transfer (*18*).

When two immiscible liquids are agitated, a dispersion is formed in which continuous breakup and coalescence of drops occurs. After some time a dynamic equilibrium is established between breakup and coalescence and a spectrum of drop sizes results. The average drop size and the size distribution will depend upon conditions of agitation as well as physical properties of the two liquids. Drops are believed (*6*) to be broken up by turbulent pressure fluctuations in the neighborhood of the drop surface. Coalescence may occur when drops collide. In a dilute dispersion coalescence will be minimal, and the equilibrium drop size distribution will depend upon the breakup process alone.

Despite the fact that the drop size distribution is a significant factor apart from its influence on the average particle size and the total interfacial area, no information exists from which one may predict the distribution function, and the manner in which it changes, with agitation parameters and physical properties of the immiscible phases. The goal of this work was to develop such information over a wide range of pertinent parameters and properties and to imbed these results within the framework of a rational theory.

A fairly extensive literature exists with regard to the average drop size obtained in dispersions. A critical discussion of this literature may be found in reference 2. Only the most pertinent references are reviewed here.

Vermeulen et al. (*21*) indirectly measured the interfacial area in liquid-liquid and gas-liquid agitated dispersions in baffled cylindrical tanks by means of a light transmission technique. A wide range of surface tensions was studied. The concentration of the dispersed phase was varied from 10 to 40%. The data could be correlated in the form

$$\overline{D}_{32}/L\phi = C_1\ N_{We}^{-0.6} \tag{1}$$

Their Weber number was based on the mean density of the mixture. Data deviated from this correlation by as much as ± 60%. Only limited geometries, two tanks of different sizes, and one impeller were employed. The inclusion of the volume fraction of dispersed phase ϕ indicates that coalescence played a role in the process.

Rodger et al. (*13*) measured average drop size in liquid-liquid dispersions using equal volumes of both liquids. Their results could be correlated by

$$\overline{D}_{32}/L = C_2\ N_{We}^{-0.36}\ (L/T)^{-k} \tag{2}$$

k varied from 0.75 to 1.4, and C_2 was found to depend upon the tank diameter T. ϕ does not appear in the correlation because only one value of ϕ was studied. However, one might expect coalescence to be a major factor for $\phi = \frac{1}{2}$, and this may explain the difference between this correlation and Vermeulen's.

Calderbank (*1*) studied interfacial area in agitated tanks with concentrations of dispersed phase ranging from nearly 0 to 20%. The variation in physical properties was limited. The results were correlated by

$$\overline{D}_{32}/L = C_3\ f_H\ N_{We}^{-0.6} \tag{3}$$

where

$$f_H = 1 + 9\phi \tag{4}$$

Equation (3) correlates the data with a maximum deviation of ± 10%. The form is quite similar to Vermeulen's correlation [Equation (1)].

Shinnar and Church (*17*) developed predictions for average particle size by using the Kolmogoroff theory of universal equilibrium (*10*). For breakup as the dominant mechanism (low values of ϕ), they obtained

$$\overline{D}_{32}/L = C_4\ N_{We}^{-0.6} \tag{5}$$

in good agreement with Calderbank's results at very small ϕ. For coalescence as an important process, they obtained a relation which can be converted to the dimensionless form

$$\overline{D}_{32}/L = C_5\ N_{We}^{-0.375} \left(\frac{A(h)}{\sigma L}\right)^{0.375} \tag{6}$$

$A(h)$ is to be thought of as an energy of adhesion between two drops of unit diameter separated by a distance h. It is some kind of coalescence parameter, apparently. Equation (6) is in partial agreement with Equation (2), which was obtained under conditions such that coalescence was probably dominant. Dependence of C_5 on L and T, as observed by Rodger, Trice, and Rushton, is not predicted by Shinnar and Church.

THE DROP SIZE DISTRIBUTION FOR DILUTE DISPERSIONS

Consider an immiscible liquid-liquid system which is in a state of agitation. The turbulent flow field may be described by an energy spectrum function $E(k)$ such that $E(k)dk$ is the energy per unit mass of continuous phase associated with fluctuations of wave number k to $k + dk$. A drop of size D is stabilized by surface energy $4\pi D^2\sigma$ and is opposed by turbulent energy $\frac{4}{3}\pi D^3\rho\varepsilon$, where

$$\varepsilon = \int_{1/D}^{\infty} E(k)\, dk \tag{7}$$

Only energy associated with fluctuations of a scale smaller than $k = 1/D$ is considered, on the grounds that larger eddies would merely carry the drop along with it, but not break it up.

The probability that a drop of size D can exist in equilibrium should be some function of the ratio of turbulent (disruptive) energy to surface (cohesive) energy, or

$$P(D) = \Phi\left[\frac{\frac{4}{3}\pi D^3\rho\int_{1/D}^{\infty} E(k)\, dk}{4\pi D^2\sigma}\right] = \Phi\left[\frac{\rho D}{3\sigma}\int_{1/D}^{\infty} E(k)\, dk\right] \tag{8}$$

where $\Phi[\ ]$ implies an unknown functional dependence.

The size range of drops, under usual conditions of interest, is such that the drop diameters are small compared with some macroscopic dimension, $D << L$, but large compared with the dissipation microscale, $D >> \eta$. These are just the conditions of applicability of Kolmogoroff's theory for the inertial subrange, the dynamics of which should control the breakup of the drops. In this range it is known that (5)

$$E(k) = \alpha\epsilon^{2/3}\, k^{-5/3} \tag{9}$$

where ϵ is the local energy dissipation rate per unit mass. Hence, the integral in Equation (8) is given by

$$\int_{1/D}^{\infty} E(k)\, dk = \frac{3}{2}\alpha\epsilon^{2/3}\ D^{2/3} \tag{10}$$

and it follows that

$$P(D) = \Phi\left[\frac{\alpha}{2}\,\frac{\rho}{\sigma}\,\epsilon^{2/3}\ D^{5/3}\right] \tag{11}$$

The dissipation rate ϵ is a local quantity which undoubtedly varies spatially throughout a stirred tank. While some measurements of ϵ exist (3), there are insufficient data upon which to base any reasonable model for ϵ as a function of position throughout the system. Instead, a weaker assumption will be made. It is assumed that at sufficiently high Reynolds numbers the form of ϵ is universal; that is

$$\epsilon(r, z, \theta)/\bar{\epsilon} = F(r/L, z/L, \theta) \tag{12}$$

where F is the same (though not necessarily known) function for geometrically similar sysems. Simply stated, Equation (12) asserts that while the spatial variation of ϵ may not be known, its variation is the same in all geometrically similar systems. Here $\bar{\epsilon}$ represents the average dissipation rate per unit mass, which is just the power input per unit mass required to agitate the system. For a well-baffled agitated tank, Rushton (14) finds

$$\bar{\epsilon} = C_6\ N^3\ L^2 \tag{13}$$

Equation (13) is valid for $N_{Re} > 10^4$.

With these assumptions it is possible to write Equation (11) as

$$P(D) = \Phi\left[\frac{D}{L}N_{We}^{0.6}\right] \tag{14}$$

If the drop size distribution can be measured, a test of Equation (14) can be made.

From $P(D)$ the average drop size follows from

$$\overline{D}_{32} = \int_o^{\infty} D^3\, P(D)\, dD \Big/ \int_o^{\infty} D^2\, P(D)\, dD \tag{15}$$

and is given by

$$\overline{D}_{32}/L = C_7\ N_{We}^{-0.6} \tag{16}$$

Equation (16), of course, is identical with the theoretical result of Shinnar and Church and is consistent with experimental data obtained with dilute dispersions.

EXPERIMENTAL WORK

A detailed discussion of the equipment and procedures is in reference 2. The major points are outlined here.

Apparatus

The major pieces of equipment consisted of a controlled variable speed power supply for the impeller; six cylindrical flat bottomed glass tanks of 4-; 6-, 8-, 10-, 12-, and 18-in. diameter, each fitted with four stainless steel baffles of width equal to one-tenth the tank diameter; five stainless steel six-blade turbine impellers of 2-, 3-, 4-, 5-, and 6-in. diameter; a light source and light transmission probe for measuring the achievement of dynamic equilibrium; and a camera and microflash for direct measurement of drop size distribution.

A schematic diagram of the equipment arrangement is shown in Figure 1. The square Plexiglas tank surrounding the system serves as a constant-temperature bath. In addition, it allows pictures to be taken through the cylindrical tank without optical distortion.

The light transmission probe was designed like that of Trice and Rodger (18). The current output from the photocell (RCA 1P41) was measured by a Leeds and Northrup galvanometer (2430C). The light source was a Bausch & Lomb Microscope Illuminator (PR-27) fitted with a heat absorbing glass filter.

Photographs were taken with a 4 by 5 Graflex camera equipped with a 135 mm. f/4.7 lens. The flash unit was a Model 549 microflash manufactured by Edgerton, Germeshausen, and Grier, Inc. It produces a 5×10^7 beam candle power flash of 0.5 μsec. duration. Kodak Contrast Process Panchromatic sheet film and D-8 developer were used for all photographic work. A 32-power traveling microscope measured individual drop diameters directly from the negatives.

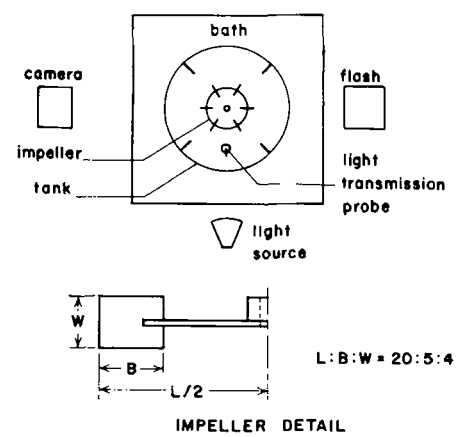

Fig. 1. Schematic diagram of the apparatus.

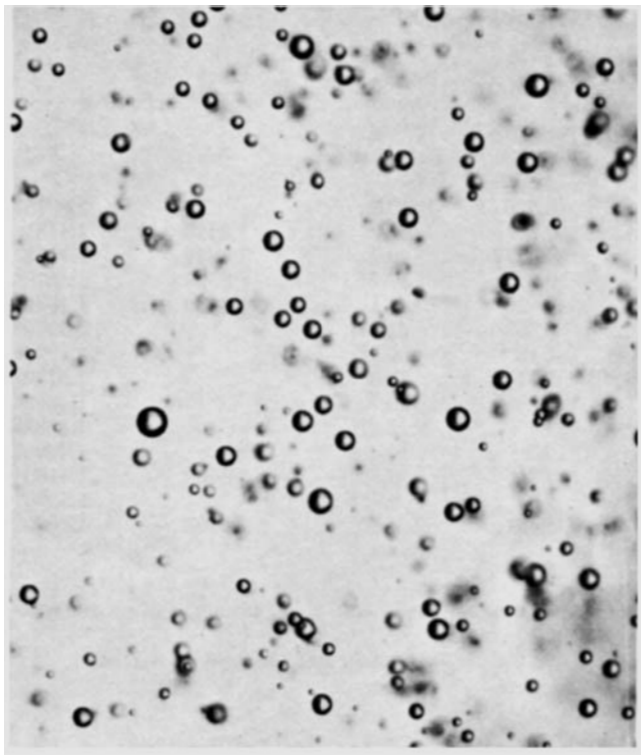

Fig. 2. Photograph of a xylene-water dispersion; $L = 6$ in., $N = 80$ rev./min., $\bar{D}_{32} = 300\ \mu$.

The photographic method was checked by preparing a mixture of glass spheres of known size distribution in the expected size range (50 to 100 μ). The spheres were agitated and photographed and the size distribution calculated. The agreement was within 5%. This experiment also indicated that a minimum count of 300 drops is necessary to obtain accurate results.

Since experiments (*4, 16*) have established a homogeneous distribution of drops throughout the agitated tank, the camera was focused on an arbitrary plane midway between the tank axis and its wall. A typical photograph is shown in Figure 2.

Procedure

The following procedure was used to obtain experimental data.

1. The glass tank was first thoroughly cleaned. It was then rinsed with distilled water followed by acetone and finally by more distilled water. The impellers and baffles were dipped into nitric acid and rinsed with water, acetone, then water.
2. The tank was filled with distilled water to a depth of 1 tank diameter and placed in the temperature bath. The vessel was centered around the impeller, leveled, and the height of the impeller from the bottom of the tank was adjusted to 1 impeller diameter. Agitation was started and adjusted to the desired impeller speed. The system was allowed to come to a constant temperature of 25°C.
3. The clean light transmission probe was inserted into the agitated tank. The position of the probe was adjusted so that a maximum reading allowable on the galvanometer was obtained when no dispersed phase was present in the tank.
4. A second liquid phase was introduced into the agitated tank with a disposable pipette. The light transmission unit was turned on to monitor the achievement of dynamic equilibrium in the dispersion. This was achieved when the galvanometer indicated a steady reading.
5. When the steady reading on the galvanometer had continued for 15 min., the probe was removed from the agitated liquids in order to avoid any influence upon the flow field caused by the presence of the probe. Agitation was continued for 15 min. more. Photographs of the dispersion were then taken. The camera apertures used were f/11 and f/16. The exposure time was set at 1/400 sec. to minimize background lighting.
6. The film was developed and dried.

Range of Experimental Variables

A tabulation of the liquid-liquid systems used appears in Table 1. Distilled water was the continuous phase. Table 2 summarizes the range of variables studied.

RESULTS

The drop size measurements were classified into size groups of either 10- or 20-μ intervals, depending upon the range of sizes resulting from each run. The Sauter mean diameter was calculated from

$$\bar{D}_{32} = \sum_{i=1}^{M} n_i D_i^3 \Big/ \sum_{j=1}^{M} n_i D_i^2 \qquad (17)$$

The Sauter mean is the most convenient average to use since interfacial area per unit volume can be calculated directly from

$$A = 6\,\phi/\bar{D}_{32} \qquad (18)$$

The size distribution was represented in terms of the volume frequency $f_v(D_i)$, defined in such a way that

$$f_v(D_i)\,dD_i = n_i D_i^3 \Big/ \sum_{i=1}^{M} n_i D_i^3 \qquad (19)$$

If $f_v(D_i)$ is identified as the function $P(D_i)$ in Equation (14), then one should expect the data to correlate as

$$f_v(D_i)\,dD_i = \Phi\left[\frac{D_i}{L} N_{We}^{0.6}\right] \qquad (20)$$

Mean Drop Size

Figure 3 shows the mean drop size correlation as $\bar{D}_{32}/L$ vs. N_{We}. The equation of the least-squares line through these data is

$$\bar{D}_{32}/L = 0.045\ N_{We}^{-0.57} \qquad (21)$$

No statistically significant effect of geometry (L/T) is observed. This seems to parallel the observation of Rushton (*14*) that the power requirement is also virtually independent of L/T in this range of Reynolds numbers.

The root-mean-square deviation of the data points (112 points in all) from Equation (21) is 17%. The 99% confidence interval on the slope is -0.515 to -0.625, which includes the theoretical value of -0.6. If the theoretical value is used, Equation (21) is replaced by

$$\bar{D}_{32}/L = 0.053\ N_{We}^{-0.6} \qquad (22)$$

Vermeulen's data, extrapolated to zero volume fraction, give a coefficient of 0.055 (*22*).

Drop Size Distribution

The volume frequency was first examined to see if the drops were distributed according to a normal distribution function. To this end, it was convenient to plot the cumulative volume frequency $F_v(D_i)$ as a function of D_i on normal probability paper. $F_v(D_i)$ is defined as

$$F_v(D_i)\,dD_i = \sum_{j=1}^{i} n_j D_j^3 \Big/ \sum_{i=1}^{M} n_j D_j^3 \qquad (23)$$

For any single run a straight line resulted, indicating normality of the distribution. However, considerable variation existed from run to run. Figure 4 shows a set of data for $L/T = 0.62$, where the ordinate has been changed to $(D_i/L)\ N_{We}^{0.60}$. No dependence of this scatter could be found with respect to any of the parameters which might be expected to affect the distribution function. It was concluded that the scatter was related to the variation of $\bar{D}_{32}$ about the line given by Equation (21). Hence, it was decided to replot the distribution function by normalizing

TABLE 1. PHYSICAL PROPERTIES OF SYSTEMS STUDIED†

System‡	Density, g./cc. ρ_c	ρ_d	Viscosity, centipoise μ_c	μ_d	Interfacial§ tension, dynes/cm. σ	Refractive index n_c	n_d
i-Octane	0.997	0.703	0.899	0.520	48.3		1.3975¶
Cyclohexane‖	0.997	0.761	0.894	0.762	46.2	1.3329	1.4181
Benzene‖	0.997	0.873	0.896	0.607	40.2	1.3332	1.4975
Chlorobenzene‖	0.997	1.101	0.890	0.776	37.7*	1.3329	1.5218
Xylene‖	0.997	0.860	0.895	0.610	36.1	1.3330	1.4942
Toluene	0.997	0.867	0.896	0.550	31.6		1.4970¶
Phenetole	0.998	0.965	0.896	1.16	39.4*		1.5076¶
Anisole	0.997	0.993	0.895	1.01	25.8*		1.5179¶
Ethyl hexanoate	0.997	0.871	0.901	1.23	20.7		1.4073¶
Oleic Acid	0.997	0.895	0.895	25.8	15.6*		1.4582¶
10-Undecenoic acid	0.996	0.908	0.890	10.3	10.4		1.4486¶
Tri-butyl Phosphate‖	0.997	0.979	0.894	3.91	8.58	1.3332	1.4169
Benzyl alcohol	1.001	1.042	1.270	5.30	4.75*		1.5396¶
Isoamyl alcorol‖	0.993	0.825	0.982	3.48	4.80	1.3362	1.4009

† Properties given are for mutually saturated phase at 25°C.
‡ In all cases the dispersed phase is indicated; the continuous phase was distilled water.
§ Experimentally determined except the ones with *; these are taken from "International Critical Table," Vol. 4, pp. 436-437, McGraw-Hill, New York (1928).
‖ Data taken from Rodger et al. (*13*).
¶ Data taken from "Handbook of Chemistry and Physics," 45 ed., C. D. Hodgman, ed., The Chemical Rubber Co., Cleveland, Ohio (1964).

the ordinate to its mean value, $(\overline{D}_{32}/L)\ N_{We}^{0.60}$. The result is shown in Figure 5. The data were similarly compressed for other values of L/T.

With the normality of $F_v(D_i)$ established, it was possible to calculate the mean and standard deviation of the distribution curve with the result that the distribution function, normalized with respect to $\overline{D}_{32}$, was given by*

$$f_v(D_i/\overline{D}_{32}) = \frac{1}{0.23\sqrt{2\pi}} \exp\left[-9.2\left(\frac{D_i}{\overline{D}_{32}} - 1.06\right)^2\right] \quad (24)$$

Again no statistically significant dependence on L/T was found. Hence Equation (24) is recommended for all geometries studied.

Figure 6 shows $f_v(D_i/\overline{D}_{32})$ plotted in the more familiar manner. A collection of data for $L/T = 0.54$, but for different values of N, L, and physical properties, is shown superimposed on the curve in order to demonstrate the scatter involved.

DISCUSSION

The major results may now be summarized. The average drop size $\overline{D}_{32}$ obeys Equation (22). This is not a new result, but rather it is a strong confirmation of previous studies which did not involve as wide a variation of parameters as the present work. The results, of course, may be used with confidence only within the range of variables presented in Table 2. It is likely that the most serious restriction is that on the volume fraction ϕ. Calderbank's results [Equation (3)] indicate that an upper limit on ϕ might be of the order of 1%.

The most significant result is the presentation of a distribution function for the volume frequency $f_v(D_i/\overline{D}_{32})$ given by Equation (24). Of particular note is the fact that the standard deviation of the curve about its mean, which is essentially a measure of the inhomogeneity of the dispersion, is independent of any of the parameters and properties studied. The standard deviation is found to be 0.23. Hence, 68% of the volume of the dispersed phase is associated with droplets whose diameters lie within ± 23% of $\overline{D}_{32}$.

Since interfacial area is a major parameter in interphase transport processes, it is convenient to have a distribution function for area. This is given by

$$f_A(D_i/\overline{D}_{32}) = \frac{\overline{D}_{32}}{D_i} f_v(D_i/\overline{D}_{32})$$

$$= \frac{\overline{D}_{32}}{0.23\sqrt{2\pi}\, D_i} \exp\left[-9.2\left(\frac{D_i}{\overline{D}_{32}} - 1.06\right)^2\right] \quad (25)$$

From this result one can show that 65% of the area of the dispersed phase is associated with droplets whose diameters lie within ± 23% of $\overline{D}_{32}$.

Considerable variability has been observed in both the mean drop size and the size distribution correlations. While the mean drop size has a precision which we estimate to be better than 10%, maximum deviations of the order of 50% are observed. In similar studies Rodger et al. (*13*)

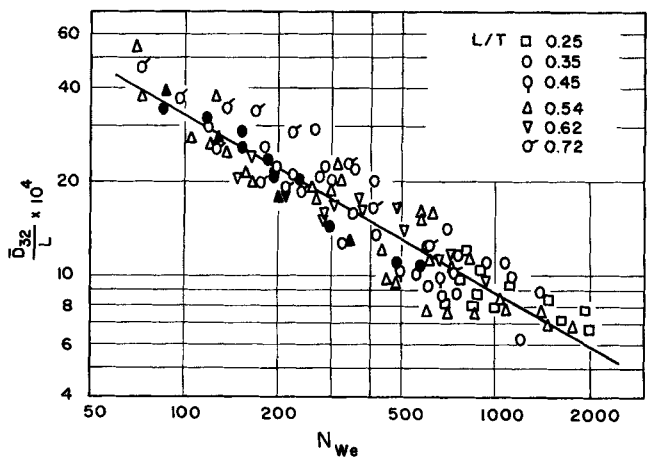

Fig. 3. Mean drop size correlation. The solid line is Equation (21). The filled-in symbols represent all of the data obtained with chlorobenzene as the dispersed phase.

* By this normalization it follows that

$$\int_o^\infty f_v\,(D/\overline{D}_{32})\ d\ (D/\overline{D}_{32}) = 1$$

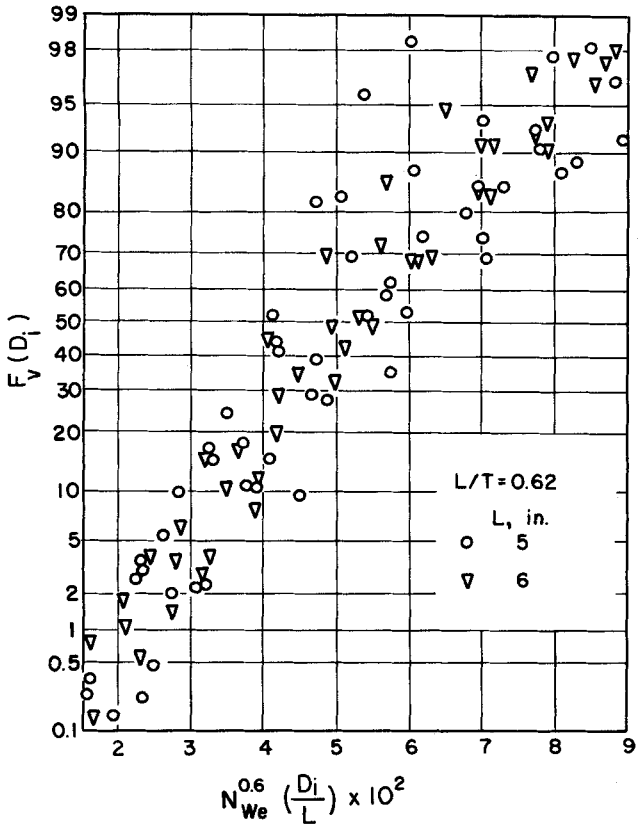

Fig. 4. Cumulative distribution function for $L/T = 0.62$.

reported an average deviation of 12% (compared with 17% in this work) and maximum deviations of 55%, while Vermeulen et al. (*21*) correlated their data with a maximum deviation of about 60%. Calderbank, whose data covered only a narrow range of physical properties, found a maximum deviation of 10%.

Rodger et al. suggested that interfacial contamination was the major factor which contributed to scatter in the data, yet noted that interfacial tension was not altered by the presence of such contamination. Of course, this may mean that they failed to identify the actual contaminant, which could possibly have been in the form of dissolved ions rather than macroscopic dirt.

A more serious suggestion is the possibility that surface tension is not a sufficient property to characterize the interface. Interfacial tension is an equilibrium property determined under static conditions and in the absence of mass transfer between phases. In some experimental runs dispersed phase was lost by evaporation from the surface. It was apparent that there was a small but steady mass transfer between phases.

Table 2. Experimental Ranges Studied

Reynolds No.	$\frac{NL^2}{\nu}$	1.2×10^4 to 10.4×10^4
Weber No.	$\frac{N^2L^3\rho}{\sigma}$	70 to 2,000
Impeller diameter	L	2 to 6 in.
Impeller speed	N	80 to 1,000 rev./min.
Tank diameter	T	4 to 18 in.
L/T ratio	L/T	0.21 to 0.73
Concentration of dispersed phase	ϕ	0.001 to 0.005

Sternling and Scriven (*19*) have discussed the promotion of interfacial turbulence by mass transfer across a phase boundary. Whether such a mechanism would be of any significance in comparison with, and in the presence of, turbulent pressure fluctuations in the neighborhood of the drop is unknown. It would appear that our present state of understanding is such that one must accept the magnitude of the variability found in this work as inherent in studies of this kind.

It is interesting to note that if the data for any single fluid are singled out (as in the case of the chlorobenzene data of Figure 3), the scatter is seen to be less than that of all of the data for all fluids. This would support the conjecture that the scatter is due to differences between fluids not completely accounted for by interfacial tension.

Often one wishes to scale up from experimental studies of dispersion in small size systems. If geometrical similarity of both the impeller and the tank is maintained, and if linear dimensions scale up from L_1 to L_2, then Equation (5) requires

$$L_1 \, N_{We_1}{}^{-0.6} = L_2 \, N_{We_2}{}^{-0.6} \tag{26}$$

if equal $\overline{D}_{32}$ is to be maintained. This leads to the condition

$$(N^3 L^2)_2 = (N^3 L^2)_1 \frac{(\rho/\sigma)_1{}^{3/2}}{(\rho/\sigma)_2{}^{3/2}} \tag{27}$$

If physical properties are the same in the model and the full scale system, and if the power input per unit mass is given by Equation (13), then Equation (27) is just the condition of equal power input per unit volume. If, for some reason of convenience, the model is run with a different dispersed or continuous phase, then the more complete expression given in Equation (27) would have to be used.

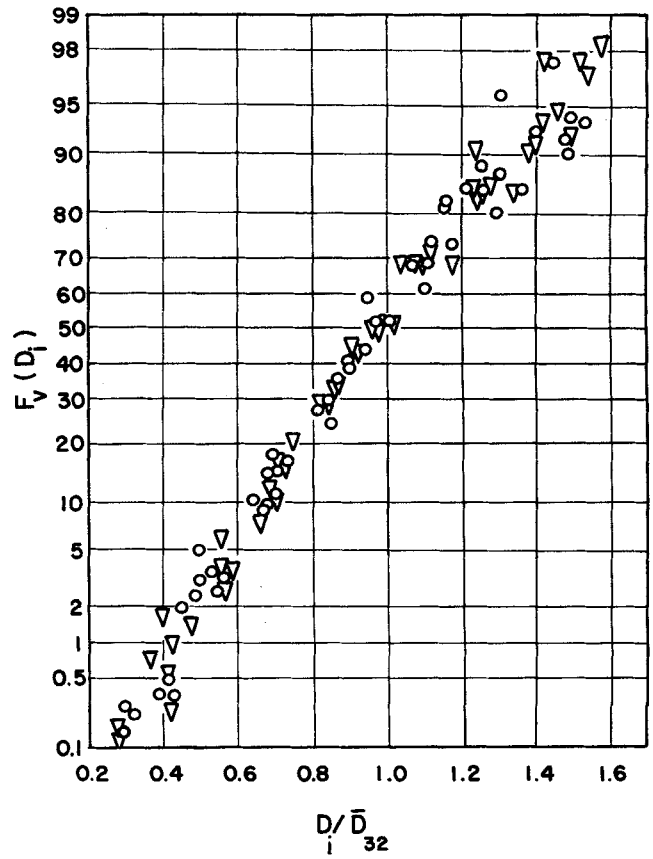

Fig. 5. Figure 4 replotted with a normalized ordinate.

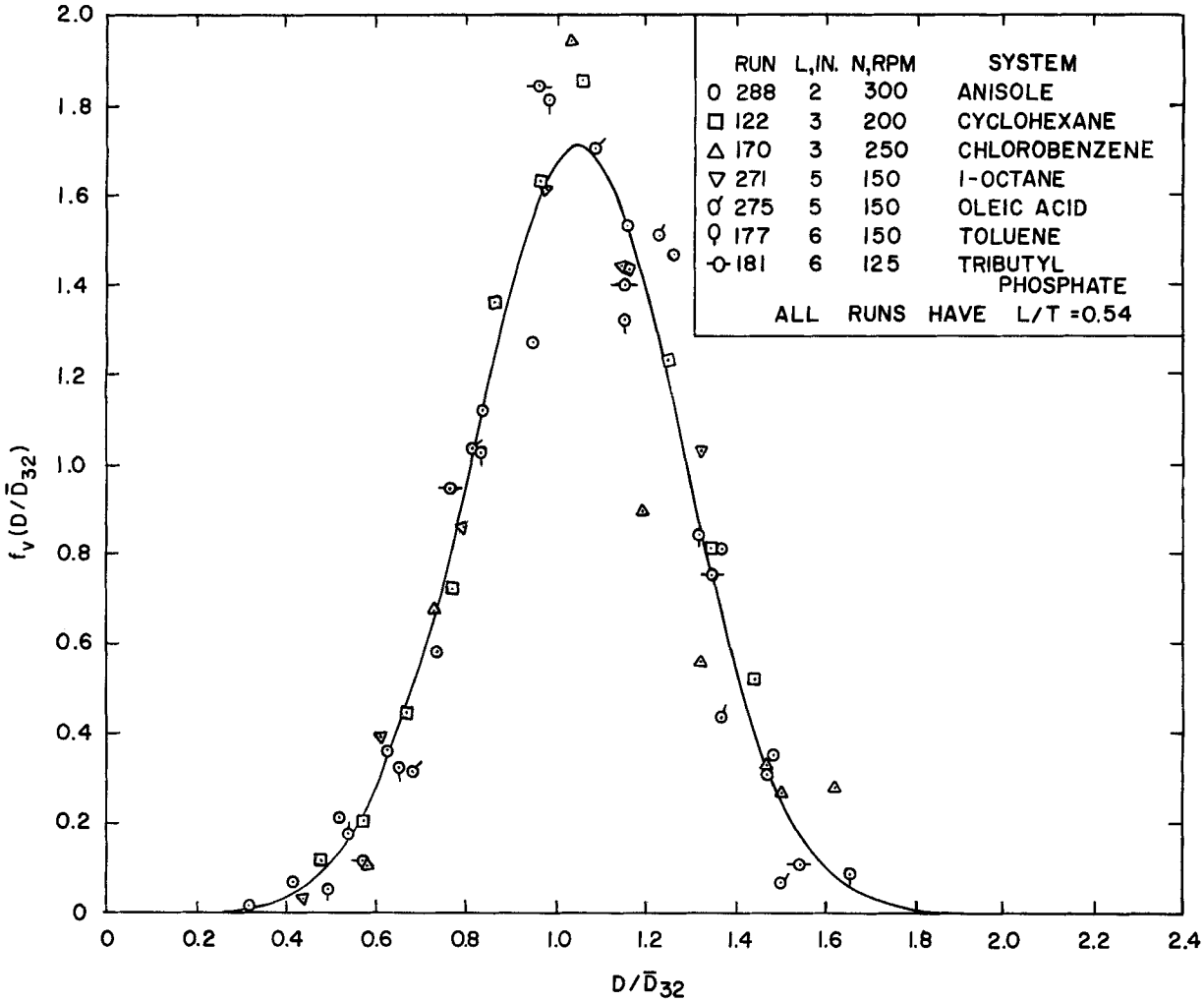

Fig. 6. The volume fraction distribution function. The solid line is Equation (24). A small sample of data is shown for comparison.

Since these results lean upon hypotheses embodied in Kolmogoroff's works, it is proper to question the applicability of the Kolmogoroff theory to this work. There is some experimental evidence (3, 9) that the energy spectrum function in an agitated tank shows behavior predicted by Kolmogoroff for the inertial subrange. There is also some evidence (11) that semiempirical theories for mass transfer from small particles based upon the Kolmogoroff hypotheses are in good agreement with experimental data obtained in turbine agitated tanks.

The conditions of applicability require that the drop sizes be very small compared with a macroscopic dimension such as L. In no case reported here was the largest drop within one order of magnitude of L. As Figure 3 shows, $\bar{D}_{32}/L$ was always in the range of 10^{-3} to 10^{-2}.

A more serious restriction is that the drops must be larger than the dissipation scale η, which is given by (5)

$$\eta = (\nu^3/\bar{\epsilon})^{1/4} \tag{28}$$

Values of η ranged from 10 to 30 μ. In the worst cases $\bar{D}_{32}$ was only four times larger than η. However, these cases do not show a significantly larger variation from the measured mean values, and it is not possible to attribute anomalous results to such a factor.

Under conditions of extremely high energy input it is possible to produce drops smaller than η. Such drops would be in a dynamic regime known as the *viscous subrange* (6). In that case Equations (14) and (16) would have to be replaced by (2)

$$P(D) = \Phi\left[\frac{D}{L} N_{We}^{1/7}\ N_{Re}^{4/7}\right] \tag{29}$$

and

$$\bar{D}_{32}/L = C_8\ N_{We}^{-1/7}\ N_{Re}^{-4/7} \tag{30}$$

It was not possible to operate under such conditions in this study, and no confirmation of these predictions is available. It is interesting to note, however, that the predictions for the viscous subrange are markedly different from those for the inertial subrange.

NOTATION

$A(h)$ = energy of adhesion between two drops separated by a distance h, (g.)(cm.)/sec.^{2}
$C_1, C_2, \ldots$ = empirical constants
D = diameter of a drop, cm.
D_i = diameter of a drop in the i^{th} size interval, cm.
$\bar{D}_{32}$ = Sauter mean diameter, cm.
$E(k)$ = energy spectrum function, cc./sec.^{2}
$f_A(D_i)dD_i$ = area fraction of drops in the i^{th} size interval
$f_v(D_i)dD_i$ = volume fraction of drops in the i^{th} size interval
$F_v(D_i)dD_i$ = cumulative volume fraction
k = wave number, cm.$^{-1}$
L = impeller diameter, cm.
M = number of size intervals

N = impeller speed, sec.$^{-1}$
N_{Re} = ND^2/ν = Reynolds number
N_{We} = $L^3N^2\rho/\sigma$ = Weber number
n_i = number of drops in the i^{th} size interval
$P(D)$ = probability that a drop of size D exists
T = tank diameter, cm.

Greek Letters

α = constant in Equation (9)
ε = turbulent energy per unit mass, defined by Equation (7), sq.cm./sec.^{2}
ϵ = local energy dissipation per unit mass, sq.cm./sec.^{3}
$\bar{\epsilon}$ = average power input per unit mass, sq.cm./sec.^{3}
η = dissipation microscale, cm.
ν = kinematic viscosity of continuous phase, sq.cm./sec.^{1}
ρ = density of continuous phase, g./cc.
σ = interfacial tension between phases, g./sec.^{2}
ϕ = volume fraction of dispersed phase

LITERATURE CITED

1. Calderbank, P. H., *Trans. Inst. Chem. Engrs.*, **36**, 443 (1958).
2. Chen, H. T., Ph.D. thesis, Univ. Rochester, N. Y. (1966).
3. Cutter, L. A., *AIChE J.*, **12**, 35 (1966).
4. Dalton, R. J., *J. Phot. Sci.*, **9**, 263 (1961).
5. Hinze, J. O., "Turbulence," McGraw-Hill, New York (1959).
6. ———, *AIChE J.*, **1**, 289 (1955).
7. Hohenstein, W. P., *Polymer Bull.*, **1**, 13 (1945).
8. ———, and H. Mark, *Polymer Sci.*, **1**, 127 (1946).
9. Kim, W. J., and F. S. Manning, *AIChE J.*, **10**, 747 (1964).
10. Kolmogoroff, A. N., *Compt. Rend. Acad. Sci. USSR.*, **30**, 301 (1941); **31**, 538 (1941); **32**, 16 (1941). English translations in "Turbulence—Classic Papers on Statistical Theory," S. K. Friedlander and Leonard Topper, ed., Interscience, New York (1961).
11. Middleman, Stanley, *AIChE J.*, **11**, 750 (1965).
12. Rietema, K., in "Advances in Chemical Engineering," T. B. Drew, ed., Vol. 5, pp. 237-302, Academic Press, New York (1964).
13. Rodger, W. A. ,V. G. Trice, Jr., and J. H. Rushton, *Chem. Eng. Progr.*, **52**, 515 (1956).
14. Rushton, J. H., E. W. Costich, and H. J. Everett, *ibid.*, **46**, 395, 467 (1950).
15. Sherwood, T. K., and R. L. Pigford, "Absorption and Extraction," McGraw-Hill, New York (1952).
16. Shinnar, Ruel, *J. Fluid Mech.*, **10**, 259 (1961).
17. ———, and J. M. Church, *Ind. Eng. Chem.*, **52**, 253 (1960).
18. Sideman, Samuel, and Zvi Barsky, *AIChE J.*, **11**, 539 (1965).
19. Sternling, C. V., and L. E. Scriven, *ibid.*, **5**, 514 (1959).
20. Trice, V. G., Jr., and W. A. Rodger, *ibid.*, **2**, 205 (1956).
21. Vermeulen, Theodore, G. M. Williams, and G. E. Langlois, *Chem. Eng. Progr.*, **51**, 85F (1955).
22. Vermeulen, Theodore, private communication.

Manuscript received May 25, 1966; revision received January 20, 1967; paper accepted January 23, 1967.

Drop Size Distributions in Strongly Coalescing Agitated Liquid-Liquid Systems

F. B. SPROW

Esso Research and Engineering Company, Baytown, Texas

Emulsion drop size distributions have been measured at various locations in a turbine mixer for the methyl isobutyl ketone-salt water system. The drop sizes are strongly dependent on the sampling position, being smallest near the impeller tip and largest at the bottom of the mixing tank. The variation of drop diameter with impeller speed has been studied and indicates that droplet breakup predominates near the impeller, whereas the coalescence of emulsion droplets can be controlling in other locations.

Many engineering operations depend on effective mass transport across liquid-liquid interfaces. The transport is, of course, strongly affected by the amount of interfacial area present in the vessel. The interfacial area is directly related to the distribution of drop sizes produced in the emulsion.

In a previous paper (7) the use of an electronic particle counter was described for the determination of complete drop size distributions in dilute (low fraction dispersed phase) agitated liquid-liquid systems. This method has been extended for use with more concentrated systems, and in the present work a mixture of 25% methyl isobutyl ketone (MIBK) and 75% salt water was emulsified in a turbine mixer. The emulsion was sampled at various locations in the mixing tank, and drop size distributions determined.

The methods of isotropic turbulence provide tools for the prediction of drop sizes in systems in which either the